Earth and Planetary Science Letters 535 (2020) 116113

Contents lists available at ScienceDirect

Earth and Planetary Science Letters

www.elsevier.com/locate/epsl

Provenance and erosional impact of Quaternary megafloods through the Yarlung-Tsangpo Gorge from zircon U-Pb geochronology of flood deposits, eastern Himalaya

Michael D. Turzewski [a,*], Katharine W. Huntington [a,*], Alexis Licht [a], Karl A. Lang [b,c]

[a] Department of Earth and Space Sciences and Quaternary Research Center, University of Washington, Seattle, WA, USA
[b] School of Earth and Environmental Sciences, Queens College, Queens, NY, USA
[c] Graduate Center, City University of New York, New York, NY, USA

ARTICLE INFO

Article history:
Received 14 September 2019
Received in revised form 31 December 2019
Accepted 18 January 2020
Available online xxxx
Editor: A. Yin

Keywords:
megaflood
Himalaya
zircon
geochronology
erosion

ABSTRACT

Holocene and Upper Pleistocene sediments in the eastern Himalayan syntaxis represent an extraordinary record of glacial outburst megafloods in one of the most tectonically active landscapes on Earth. Glacial damming and outburst floods in the syntaxis may have focused erosion in the steep Tsangpo Gorge and inhibited river incision into the margin of the Tibetan Plateau. However, few flood slackwater deposits have been studied, and it is unknown which of the hundreds of known glacial impoundments in Tibet may have sourced the floods. Here we report n=1438 new detrital zircon U-Pb data from individual ancient megaflood and historical outburst flood slackwater deposits to examine the provenance and erosive potential of these events. Detrital zircon U-Pb geochronology of megaflood deposits show that megaflood provenance is more consistent with impoundment of the Yarlung River drainage at or west of the Namche Barwa massif, than impoundment of eastern drainages along the Yigong and Parlung Rivers. Compared to active bedload in the Siang River, and historical floods within the same drainage area, megaflood samples overall contain a disproportionately large amount of zircons eroded from the Tsangpo Gorge. We interpret this preferential derivation to reflect preferential erosion during large discharge events—supporting the hypothesis that Quaternary megafloods are a primary contributor to rapid exhumation of the eastern Himalayan syntaxis.

1. Introduction

The contribution of extreme events such as earthquakes, landslides, and outburst floods to the long-term erosion and landscape evolution on Earth and on Mars is debated (e.g., Lamb et al., 2008; Lamb and Fonstad, 2010; Lang et al., 2013; Perron and Venditti, 2016; Larsen and Lamb, 2016). Bedrock rivers respond to perturbations in climate and tectonics to drive landscape evolution (Whipple et al., 2013), and recent work has highlighted important connections between outburst floods of different magnitudes, bedrock incision, lateral erosion, and hillslope processes (Turowski et al., 2008; Larsen and Montgomery, 2012; Turzewski et al., 2019). However, we lack direct observations of the largest magnitude flood events on Earth and must rely on numerical simulations and information about these events stored in sedimentary and geomorphic archives.

The eastern Himalaya contains a rich geomorphic and sedimentary record of outburst floods in its rugged landscape (Fig. 1). Widespread geomorphic evidence records glacial damming (e.g., Montgomery et al., 2004; Liu et al., 2006; 2015; 2018; Korup and Montgomery, 2008; Kaiser et al., 2010; Guangxiang and Qingli, 2012; Zhu et al., 2013; 2014; Huang et al., 2014; Chen et al., 2016; Hu et al., 2018), and outburst megafloods with discharges >10^6 m^3/s sourced from such impoundments in Tibet (Montgomery et al., 2004; O'Connor et al., 2013; Srivastava et al., 2017). In addition to experiencing high peak annual flows (10^4 m^3/s; Goswami, 1985), rivers in the region also experience century-scale landslide-dam outburst floods (10^5 m^3/s; Delaney and Evans, 2015), resulting in a high capacity for erosion throughout the Holocene and Late Pleistocene (e.g., Larsen and Montgomery, 2012; Lang et al., 2013; Turzewski et al., 2019). Sediment eroded from the Himalaya during megafloods includes biospheric particulate or-

* Corresponding authors.
E-mail addresses: zewski@uw.edu (M.D. Turzewski), kate1@uw.edu (K.W. Huntington).

https://doi.org/10.1016/j.epsl.2020.116113
0012-821X/

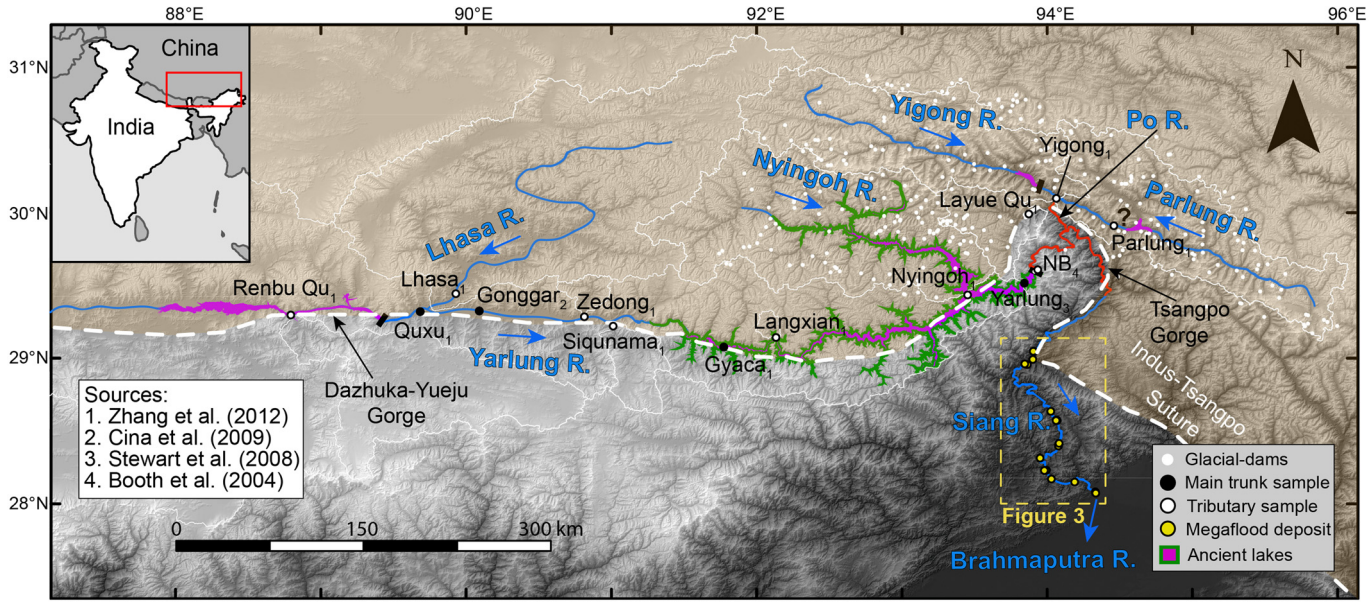

Fig. 1. Location map of study area as a hillshade over topography (SRTM3 digital elevation model). The Yarlung River flows into the Tsangpo Gorge (red) from the west, and the Yigong and Parlung Rivers flow into the Gorge through the Po River from the north. Zircon age distributions in the study area are characterized by detrital samples from the main trunk Yarlung River, tributaries to the Yarlung, and the Yigong and Parlung Rivers; and from bedrock data from Namche Barwa. Drainage areas for the detrital zircon samples are outlined in white. Locations of dated ancient megaflood deposits (Lang et al., 2013; this study), reconstructed glacially-impounded lakes (Montgomery et al., 2004; Hu et al., 2018; see text), and glacial dams mapped between 92 and 96°E by Korup and Montgomery (2008) are also shown. (For interpretation of the colors in the figure(s), the reader is referred to the web version of this article.)

ganic carbon that is deposited and buried in the Bay of Bengal, making these events relevant to the global carbon budget in one of the largest river deltas in the world (Galy et al., 2015).

Previous workers have used detrital zircon geochronology and thermochronology as a tracer for erosion in the Tsangpo Gorge (Stewart et al., 2008; Enkelmann et al., 2011; Lang et al., 2013). Detrital zircon U-Pb core crystallization ages from four slackwater deposits (n=450) presented in Lang et al. (2013) suggest that megafloods have a different signature of erosion on the landscape than sediment traveling in the modern river bedload and sediment derived from a historical landslide-dam outburst flood on the Yigong River (Shang et al., 2003; Delaney and Evans, 2015), consistent with disproportionate derivation from the Tsangpo Gorge.

This intriguing result highlights the important role of megafloods in the evolution of this landscape, and demonstrates the utility of detrital zircon U-Pb geochronology as an erosional tracer for comparing the erosional impact of variable discharges within the same drainage area. Here we expand on this work to investigate megaflood sources and variability among individual event deposits with 1438 new zircon U-Pb age data from modern/historical outburst flood and megaflood slackwater deposits. We combine these data with previously reported zircon ages for flood and fluvial deposits and source regions within the Siang-Brahmaputra drainage to examine the role of impoundment location and sediment recycling on detrital zircon U-Pb age distributions in megaflood deposits; constrain potential flood source regions in Tibet; and evaluate the hypothesis that Quaternary megafloods reflect greater preferential erosion of Tsangpo Gorge compared to what is observed in modern river flows.

2. Background

2.1. Potential source regions of megafloods through the eastern Himalaya

Megafloods through the Tsangpo Gorge could have been sourced from any of hundreds of paleo-lake impoundments that have been mapped within the upstream drainage area in Tibet (Fig. 1; Korup and Montgomery, 2008; Korup et al., 2010). The rugged pathways of the Yarlung and Po Rivers meet in between the peaks of Gyala Peri (7294 m.a.s.l.) and Namche Barwa (7782 m.a.s.l.) in the Tsangpo Gorge (Fig. 1). The Yigong and Parlung Rivers are upstream of this confluence to the northeast; upstream of this confluence to the west, the Yarlung River drainage contains an extensive network of tributaries including the Nyingoh and Lhasa Rivers (Fig. 1). In this paper, we refer to glacial-lake impoundments to the northeast of the Namche Barwa massif on the Yigong and Parlung Rivers as eastern Tibetan sources, and impoundments at and to the west of Namche Barwa on the Yarlung River as western Tibetan sources.

Several Holocene and Upper Pleistocene impounded paleolakes have been documented on the Yarlung River, representing potential western Tibetan sources for megafloods that would have traveled through the Tsangpo Gorge and into the Siang River valley in India (Montgomery et al., 2004; Liu et al., 2006; Korup and Montgomery, 2008; Kaiser et al., 2010; Zhu et al., 2013, 2014; Huang et al., 2014; Liu et al., 2015; Chen et al., 2016; Hu et al., 2018; Liu et al., 2018). Impoundment of the Yarlung River immediately upstream of Namche Barwa produced at least two lakes during the last 13 ka (Fig. 1). Holocene lake terraces dated at 1160-1574 cal yr B.P. correlate to glacial-moraine dams near the entrance of the Tsangpo Gorge at Namche Barwa, recording a ~81 km^3 paleolake, the failure of which produced a flood with an estimated peak discharge of 1×10^6 m^3/s (Montgomery et al., 2004). A second set of terraces dating to 9997-11,285 cal. yr B.P. may correspond to a larger, 835 km^3 reconstructed lake thought to have produced an estimated peak discharge of 5×10^6 m^3/s in a catastrophic flood (Montgomery et al., 2004). However, other terraces in the area show that this larger lake may have existed in several stages at different maximum elevations (Montgomery et al., 2004; Liu et al., 2006; Zhu et al., 2013; Huang et al., 2014), and various dated lacustrine sediments up to 75 ka B.P. are difficult to correlate to one another (Montgomery et al., 2004; Liu et al., 2006; 2015; Huang et al., 2014).

Further upstream and to the west in the middle reaches of the Yarlung River there is evidence of a prolonged glacial-

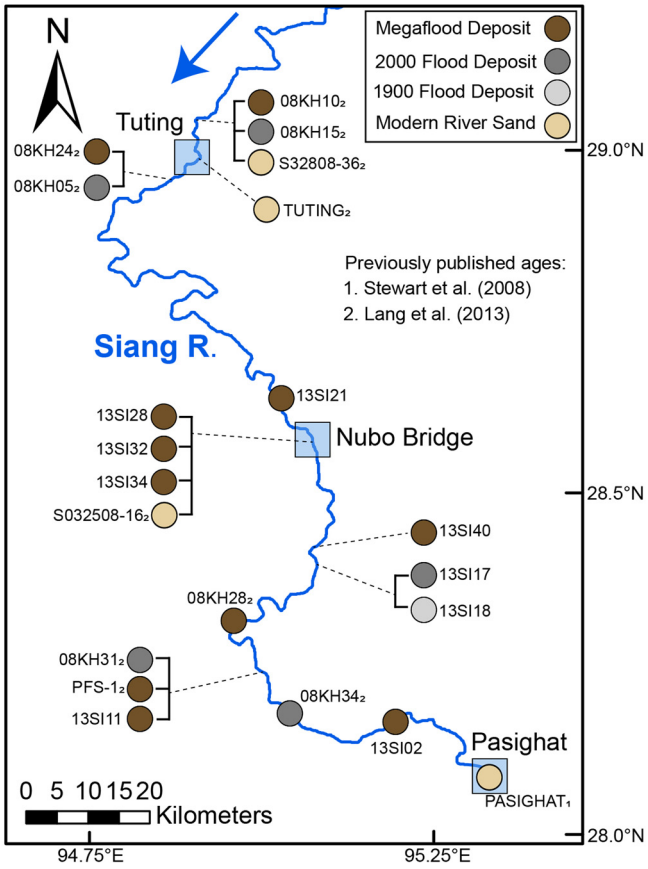

Fig. 2. Sample locations along the Siang River, northeast India, showing previously dated flood slackwater samples (Lang et al., 2013) and modern river detritus (Stewart et al., 2008; Lang et al., 2013), and new samples collected in this study.

impoundment (32.3 to 13.2 cal. ka B.P.) and resulting flood above the Dazhuka-Yueju Gorge (Kaiser et al., 2010; Zhu et al., 2013; Hu et al., 2018; Fig. 1). The catastrophic failure of this lake is supported by field evidence of coarse gravels and boulders near the Dazhuka-Yueju Gorge (Hu et al., 2018); estimates of the timing of a flood include constraints from luminescence (12.8 to 13.5 ka; Kaiser et al., 2010; Zhu et al., 2013; Hu et al., 2018) and radiocarbon dating (13.2 ka B.P.; Hu et al., 2018) of the topmost lacustrine sediments, and may be related to warming in the region during the Bølling-Allerød period (Hu et al., 2018).

In addition to impoundment of the main stem Yarlung River, dams may have temporarily blocked northward flowing Yarlung tributaries upstream of the gorge (Burrard and Hayden, 1907). Zhang et al. (2016) proposed that ice dams blocking the Siqunama River may have led to localized lake spillover into the Subansiri River valley. Lake spillover into the Subansiri River valley would have been contained within a separate drainage basin southwest of our study area, and cannot explain deposition of the Siang River valley samples in this study.

Hundreds of potential glacial-moraine dams have been mapped on eastern Tibetan tributaries of the Yigong and Parlung Rivers upstream of the Po-Tsangpo Gorge (Fig. 1; Korup and Montgomery, 2008; Korup et al., 2010). However, exposures of paleo-lake sediments in this region are sparse and are limited to a few lacustrine terraces identified on the Parlung River, which date from 16.1 to 22.5 ka B.P. (Guangxiang and Qingli, 2012).

It is unknown whether ancient slackwater flood deposits downstream of the Tsangpo Gorge along the Siang River valley (Fig. 2) record megaflood events sourced from eastern Tibetan impoundments and/or western Tibetan impoundments in the Yarlung River drainage at or upstream of the Namche Barwa massif. Here we use variations in detrital zircon U-Pb crystallization ages to discriminate between potential source regions in Tibet.

2.2. Constraints on source-region zircon U-Pb ages

Tectonic terrains involved in the collision of the Indian and Eurasian plates produce distinct patterns of zircon crystallization ages in bedrock eroded by the Yarlung-Siang-Brahmaputra River system (Booth et al., 2004, 2009; Cina et al., 2009; Gehrels et al., 2011; Lang et al., 2013; Hu et al., 2018). Of the detrital zircon ages that characterize the bedrock of this region, the less than ~1000 Ma ages (Fig. 3, Table 1) include contributions from Himalayan zircons (~300-750 Ma, with a peak probability density at ~490 Ma; Stewart et al., 2008; Cina et al., 2009; Amidon et al., 2005); Tibetan zircons (<300 Ma; Cina et al., 2009; Zhang et al., 2012); and anatectic zircons from Himalayan rock of the Namche Barwa massif/Tsangpo Gorge specifically that are distinguished by their young crystallization ages (<30 Ma; Booth et al., 2009) and high U/Th ratios (>10; see Lang et al., 2013).

Previously published detrital zircon data from the source region (n=2299) are summarized in Figs. 1–4, and Tables 1 and 2. Western Tibetan sources are characterized by detrital zircon ages from the main trunk of the Yarlung River and its tributaries (Fig. 3). Main trunk Yarlung River samples west of the Tsangpo Gorge are generally dominated by a narrow ~50 Ma age peak representing Paleogene igneous rocks; a few 100-220 Ma zircons sourced from Cretaceous to upper Triassic volcanic and sedimentary rocks; and a minor component of 400-750 Ma zircons from Paleozoic to late Proterozoic rock of the Greater Himalayan Sequence south of the Indus-Tsangpo suture, sourced from tributaries that flow north into the Yarlung River (Stewart et al., 2008; Cina et al., 2009; Zhang et al., 2012). We note that while ~50 Ma zircons are generally diagnostic of western Tibetan sources due to their abundance in Yarlung River samples, zircons in this age range may also be sourced from transhimalayan plutonic units northeast of the gorge (Zhang et al., 2012; Lang and Huntington, 2014). Age distributions of tributaries to the Yarlung River farther upstream in the middle reaches of the drainage are more variable, and generally contain age peaks <250 Ma as well as contributions of ~500-750 Ma zircons plus or minus other age components. Zircon ages from the Tsangpo Gorge and Namche Barwa massif have two peaks at 27 Ma and 490 Ma (Booth et al., 2004; 2009; Zhang et al., 2012). Cenozoic ages reflect anatectic zircons with U/Th ratios >10 (Lang et al., 2013) whereas 490 Ma ages reflect recycled ages derived from Indian crust. Zircons from tributaries entering the Gorge through the Po River from eastern Tibetan sources are mostly ~100-220 Ma in age, with some ~45-75 Ma and few >220 Ma zircons.

2.3. Detrital zircon U-Pb geochronology of modern Siang River sediments and historical outburst flood deposits

Detrital samples from the Siang River integrate the Tibetan and Himalayan source age distributions described above (Fig. 2, 4). Most zircons from samples representative of the modern Siang River are distributed between 50 Ma and 350-550 Ma (Stewart et al., 2008; Lang et al., 2013). These authors argued that the large proportion of 350-550 Ma zircons (~47%) from just 2% of the total upstream drainage reflects localized, extreme erosion of the Tsangpo Gorge area.

Zircon age distributions of slackwater deposits from the 2000 Yigong River landslide-dam outburst flood sampled up to 30 m above the Siang River channel by Lang et al. (2013) differ slightly from those of modern Siang River sediments (Fig. 4). The youngest age peak in these Yigong flood deposits is ~66 Ma, older than the ~50 Ma peak that characterizes Yarlung River source samples and modern Siang River detritus. The Yigong flood deposits also

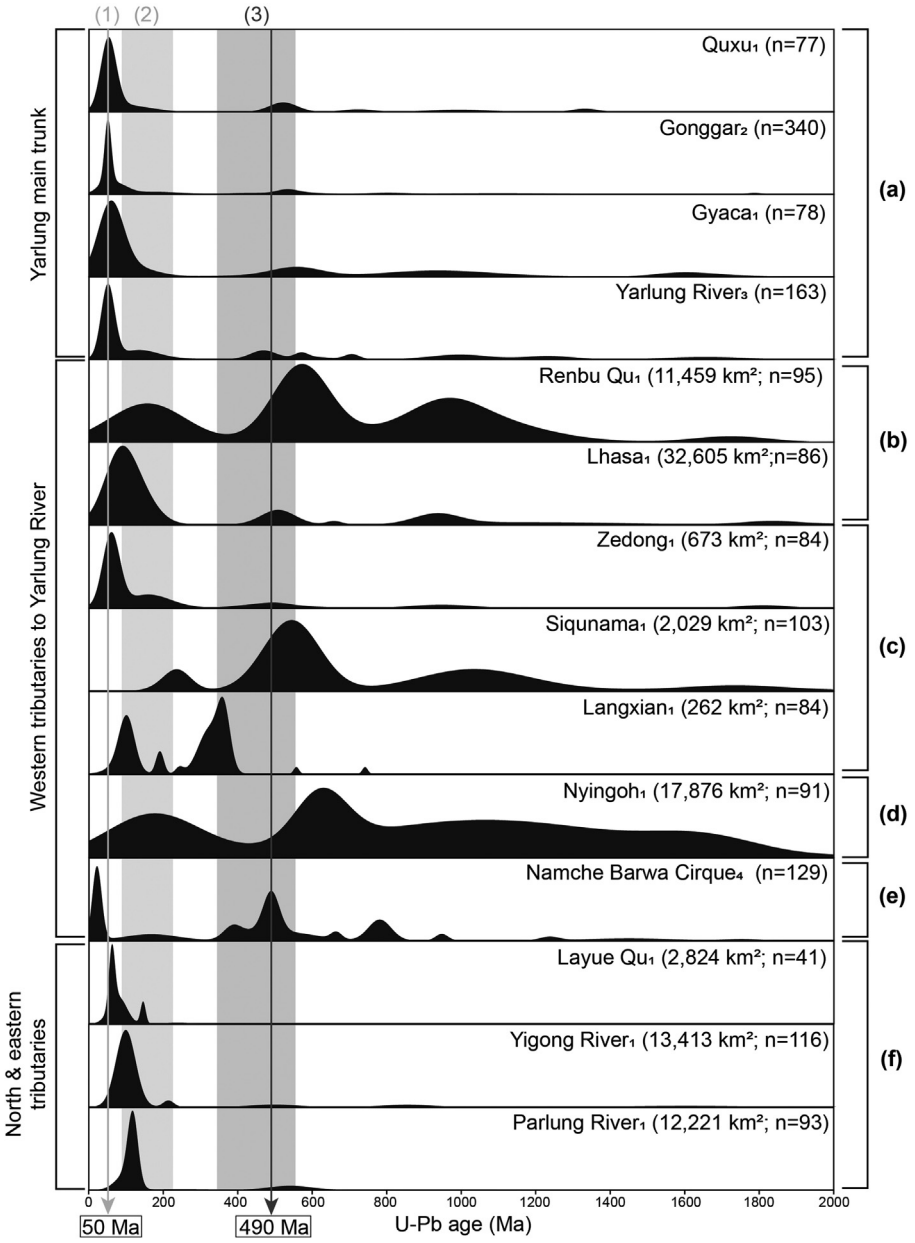

Fig. 3. Zircon age distributions of previously published samples that characterize some potential source regions in this study (sample locations and references shown in Fig. 1). Kernel density estimate (KDE) plots show data for (a) Yarlung River main trunk detrital samples; (b-d) detrital samples from western tributaries to the Yarlung; (e) bedrock samples from Namche Barwa; and (f) detrital samples from northern and eastern Tibetan sources of sediment. Line (1) represents the age peak at ~50 Ma that is characteristic of the Yarlung River source samples (a), and line (2) represents the age peak at ~490 Ma that is characteristic of Namche Barwa bedrock. Sources for detrital samples include: Zhang et al. (2012)$_1$, Cina et al. (2009)$_2$, Stewart et al. (2008)$_3$. The bedrock data are from Booth et al. (2004)$_4$.

contain 350-550 Ma Himalayan-age zircons like the modern Siang River samples, and ~100-220 Ma zircons representing the Yigong River age signature (Fig. 3).

Detritus from four ancient megaflood slackwater deposits sampled up to 150 m above the modern Siang River channel by Lang et al. (2013) (n=450) contains more ~350-550 Ma zircons that are characteristic of the Tsangpo Gorge compared to the modern Siang River and Yigong flood samples (Fig. 4). Based on forward mixture modeling of these and previously published source-region zircon data, Lang et al. (2013) argued that megafloods disproportionately focused erosion in the Tsangpo Gorge compared to these smaller magnitude flows. Building on this previous work, we sampled and analyzed additional flood deposits in the Siang River valley to explore the potential influence of flood provenance, erosion, and sediment recycling on detrital age signals.

3. Methods

3.1. Slackwater flood deposit identification and sample collection

The n=1438 new detrital zircon U-Pb data reported here come from two historical landslide-dam outburst flood samples, one reported here for the first time and one described by Turzewski et al. (2019), and seven new ancient megaflood samples described here for the first time (Fig. 2; Table 2). All samples were collected in northeast India during fieldwork performed in 2013. Sample locations for these deposits, as well as previously published samples of Lang et al. (2013) are shown in Fig. 2 and Table 2.

Flood deposits were distinguished from fluvial and landslide deposits based on their sedimentary features and position, following Lang et al. (2013) and Turzewski et al. (2019). Ancient flood deposits are exposed in roadcuts above the Siang River and near

Table 1
Previously published zircon U-Pb samples characterizing Tibetan source areas.

Sample name	Lat [DD]	Lon [DD]	Number of analyses (n)	Reference
Quxu	29.3193	90.6864	77	Zhang et al., 2012
Gonggar	29.3228	91.0921	340	Cina et al., 2009
Gyacca	29.0747	92.7748	78	Zhang et al., 2012
Yarlung R.	29.3228	91.0921	163	Stewart et al., 2008
Renbu Qu	29.2959	89.7952	95	Zhang et al., 2012
Lhasa	29.4426	90.9315	86	Zhang et al., 2012
Zedong	29.2837	91.8158	84	Zhang et al., 2012
Siqunama	29.219	92.0144	103	Zhang et al., 2012
Langxian	29.141	93.135	84	Zhang et al., 2012
Nyingoh	29.4333	94.4543	91	Zhang et al., 2012
Namche Barwa Cirque	29.60642	94.93687	129	Booth et al., 2004
Layue Qu	29.9888	94.875	89	Zhang et al., 2012
Yigong R.	30.0967	95.0647	116	Zhang et al., 2012
Parlung R.	29.9084	95.4606	94	Zhang et al., 2012

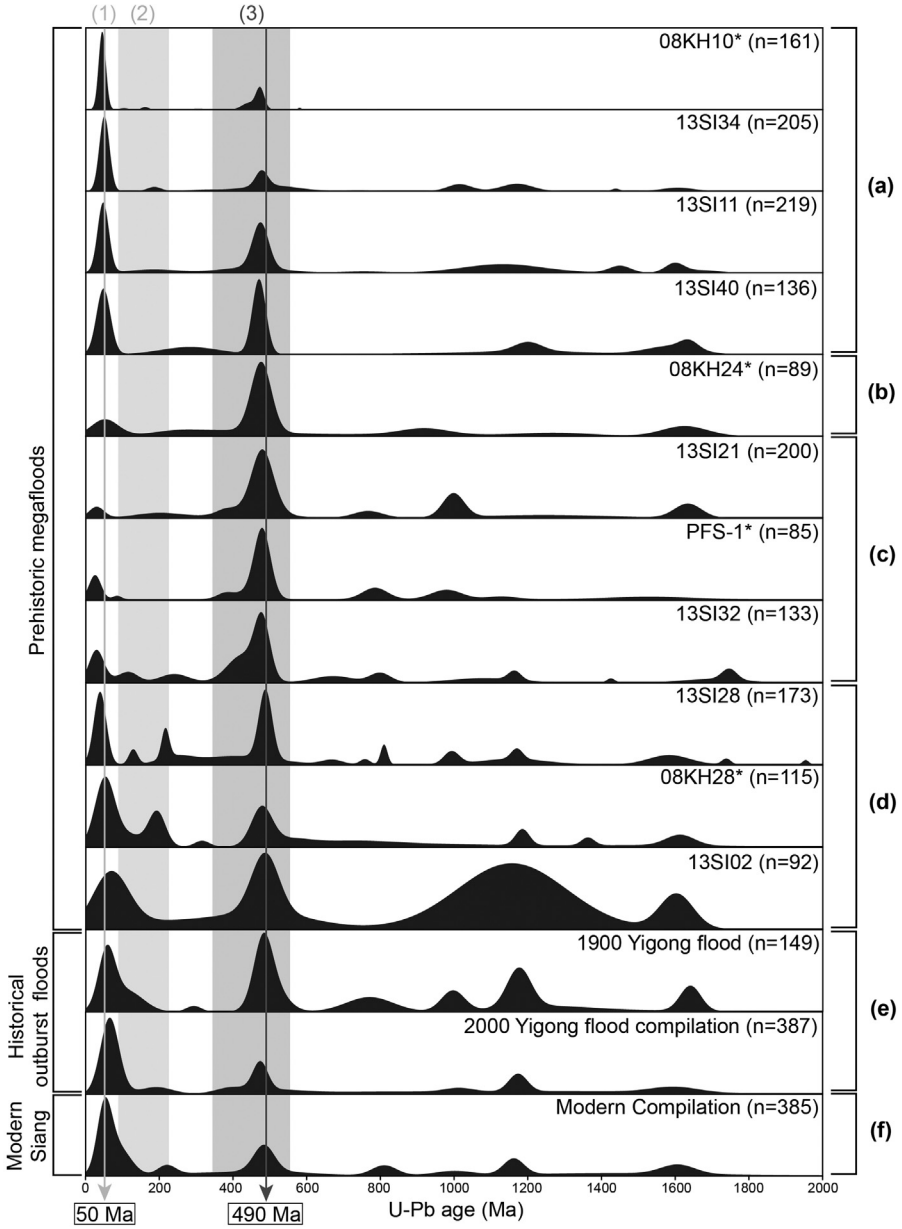

Fig. 4. Detrital zircon age distributions from Siang River valley samples, including (a-d) ancient megaflood deposits from this and previously work (* indicates previously published data of Lang et al., 2013); (e) slackwater deposits from historical landslide-dam outburst floods including a new 1900 Yigong flood sample (this study) and the updated 2000 Yigong flood data compilation (Lang et al., 2013; this study); and (f) published modern Siang River sample compilation (Stewart et al., 2008; Lang et al., 2013).

Table 2
Samples from slackwater flood deposits.

Sample name	Deposit type	Grain size (D50) [mm]	Lat [DD]	Lon [DD]	Elevation [m]	Number of analyses (n)
13SI02	Megaflood	0.512	28.1533	95.19072	555	92
13SI11	Megaflood		28.23355	94.98277	271	215
13SI40	Megaflood		28.41904	95.08376	309	135
13SI28	Megaflood	0.164	28.5763	95.06302	427	164
13SI32	Megaflood	0.240	28.57915	95.06281	400	133
13SI34	Megaflood	0.253	28.57959	95.06693	360	200
13SI21	Megaflood		28.63944	95.02667	394	200
08KH10[1]	Megaflood		29.051366	94.906178	502	161
08KH24[1]	Megaflood		28.965522	94.847082	553	89
08KH28[1]	Megaflood		28.317589	94.95328	353	115
PFS-1[1]	Megaflood		28.233917	94.983443	270	85
13SI17	1900 Yigong flood		28.40177	95.07956	278	149
13SI18	2000 Yigong flood		28.40177	95.07956	279	131
08KH34[1]	2000 Yigong flood	0.140	28.173515	95.030536	199	42
08KH31[1]	2000 Yigong flood		28.235035	94.996516	230	113
08KH05[1]	2000 Yigong flood	0.355	28.960825	94.865067	466	44
08KH15[1]	2000 Yigong flood	0.167	29.048683	94.910801	475	57
SC03-26-08-(6)[2]	Modern Siang River		28.0768	95.3356	156	137
S032508-16[1]	Modern Siang River		28.576655	95.070195	264	88
TUTING[1]	Modern Siang River		28.996279	94.903436	425	58
S032808-36[1]	Modern Siang River		29.048474	94.910787	449	73

Superscripts indicate previous detrital samples of Lang et al. (2013)[1] and Stewart et al. (2008)[2].

major tributaries that inundate during floods. One slackwater deposit from the 2000 Yigong flood that was identified in a previous field season was observed in 2013 to have been covered by a small landslide, illustrating a mechanism by which ancient flood deposits may be preserved in this rapidly eroding landscape. In several locations, deposits from multiple megaflood events were located in stratigraphic succession, in some cases separated by landslide deposits.

We analyzed zircons from two slackwater flood deposits interpreted to represent deposition from historical landslide-dam-break outburst floods on the Yigong River (e.g., Delaney and Evans, 2015). The 2000 Yigong flood sample (13SI18) was mapped by Turzewski et al. (2019) 48 m above the modern river at low flow. This deposit is composed of laminated fine to medium grain sand, shows no signs of soil development, and has small <0.5 m vegetation growth on top. Sample 13SI17 is from a laminated deposit with similar grain size, that is located on a surface 1-2 m lower in elevation than the 2000 flood deposit and is capped by thick vegetation including a ~40 cm diameter jackfruit tree at least 50-70 years old. The age of this tree and the characteristics of this deposit suggest deposition by the 1900 Yigong River outburst flood (Fig. S2).

The seven new megaflood deposits (Fig. 2) are located 72-381 m above the modern Siang River level at low-flow. The highest deposit (13SI02) exposure is approximately 90 m long and 6 m thick, making it the largest deposit identified in the field (Fig. S3). Samples 13SI21 and 13SI40 are from deposits on terraces >70 m above the river level exposed in roadcuts and are 1-2 m thick (Fig. S4; S5). The remaining samples are from vertical sequences of slackwater megaflood deposits separated by landslide colluvium (Fig. S6). Three of the deposits (13SI28, 13SI32, 13SI34) are 96-163 m above the river on a series of terraces near Nubo Bridge, which was destroyed during the 2000 Yigong flood (Fig. S7; S8). For reference, at this location, deposits from the 2000 Yigong flood are located at 35 m above the river level.

3.2. Detrital zircon sample preparation and U-Pb geochronology

For each sample, approximately 1-2 kg of fine-medium sand was processed with standard mineral separation techniques. Samples were sieved to isolate the 80-250 µm size fraction, which is a size-range that is typical of the sand observed in deposits (Table 2). Zircons were separated with a Wilfley table, lithium polytungstate and diiodomethane heavy liquids, and a Frantz magnetic separator. Although the Wifley table and magnetic separator are a standard method to extract zircons, we note that they may introduce bias (Sircombe and Stern, 2002; Vermeesch et al., 2017). Zircons were mounted, polished, and imaged with backscattered electron imaging (Hitachi 3400N SEM) at the University of Arizona. Zircon cores were analyzed for U-Th-Pb geochronology with laser ablation multi-collector inductively coupled mass spectrometry (LA-MC-ICPMS) using a 30 µm spot diameter at the Arizona LaserChron Center (Gehrels et al., 2011). U-Pb age data were reduced using NUPMagecalc and ISOPLOT using standard age filters. Additional information about preparation, analysis, and reduction of data is available in Pullen et al. (2014).

3.3. Statistical analysis of detrital provenance

We compared zircon U-Pb age distributions from the new and previously published samples using a variety of statistical methods. Zircon age distributions are presented as kernel density estimates (KDE) fitted with automatic selection of bandwidth (Botev et al., 2010). We also used multidimensional scaling (MDS) to quantify similarity among the age distributions of different samples (Vermeesch, 2013); this method has been shown to be a useful tool for examining similarity in detrital datasets in a variety of geological applications (e.g., Vermeesch, 2013, 2018; Vermeesch and Garzanti, 2015; Licht et al., 2016; Makuluni et al., 2019). Detrital provenance was further investigated via Bayesian inversion of zircon age distributions, which uses the information in the downstream detrital sample to search for age components and their characteristics.

Inversions were performed with BayesMix software (Jasra et al., 2006; Gallagher et al., 2009), which has been used by previous workers to distinguish tectonic terrains and analyze the provenance of loess and paleosol deposits (e.g. Licht et al., 2016; Perrot et al., 2017). BayesMix uses a reversible jump Markov chain Monto-Carlo (RJ-MCMC) sampling strategy to select the age, width, and number of individual components, and the proportion of each component present in sample age distributions. We ran BayesMix with 20,000 iterations assuming heavy skew-t distributions for priors and compared the age, error, and proportion of all components from each sample. The inversion was performed on compilations of detrital zircon data from geologically equivalent deposits recording the same event/processes including five 2000 Yigong

outburst flood deposits (n=387), and four modern Siang river samples (n=356). We performed inversions on a compilation of all 11 megaflood deposits (n=1608) and on sub-groups of similar megaflood samples.

4. Results

4.1. Detrital zircon U-Pb geochronology results

Zircon U-Pb data from the n=1438 new analyses presented here are available in Table S1 of the supplementary information. Fig. 4 presents zircon age distribution KDEs for seven new and four previously reported megaflood samples (Lang et al., 2013); one new 1900 Yigong flood sample; the 2000 Yigong flood sample compilation (data from Lang et al. (2013) and sample 13SI18 from this study); and the compilation of modern Siang River sample data (Stewart et al., 2008; Lang et al., 2013).

All megaflood deposits have a ~490 Ma age peak corresponding to the prominent age peak in the Namche Barwa/Tsangpo Gorge source sample (Fig. 3, 4). The relative magnitude of the ~490 Ma peak, as well as the position, width, and relative magnitude of the youngest age peak varies among deposits. Four of the megaflood deposits (group 1) have a youngest age peak at ~50 Ma (Fig. 4a, b), corresponding to the youngest age peak observed in western Tibetan source samples along the main trunk of the Yarlung River (line 1 in Fig. 3); a fifth sample (08KH24; Fig. 4b) has a similar youngest age peak that is broader and relatively smaller than those of the other samples in group 1. Three of the deposits (group 2) have a youngest age peak (Fig. 4c) that matches the ~27 Ma youngest age peak in the Namche Barwa source sample that represents anatectic zircons (Fig. 3, 6). Three deposits (group 3) have youngest age peaks in the ~25 to 65 Ma range and also contain prominent age peaks from ~100-220 Ma (Fig. 4d) that may correspond to eastern Tibetan sources of the Yigong and Parlung Rivers or tributaries of the middle-reaches of the Yarlung River to the west (Fig. 3).

The new 1900 Yigong flood sample and updated 2000 Yigong flood sample compilation share an age peak at ~490 Ma similar to the megaflood samples, but have a youngest age peak around ~66 Ma with positive skew toward older ages (Fig. 4e). When the new megaflood sample data are combined with the previously published megaflood zircon data of Lang et al. (2013), the compiled dataset support the previous hypothesis that megaflood sediments contain more zircons from the Tsangpo Gorge (bar 3) compared to the modern Siang River and 2000 Yigong flood sample compilations (Fig. S9).

4.2. MDS similarity results

The MDS map (Fig. 5) plots dissimilarity among detrital samples representing source areas in Tibet and the Tsangpo Gorge, modern Siang River sediment and Yigong flood deposit data compilations, and individual megaflood deposits. The overall stress value of the map is 0.10283, between a fair and good fit to the data (Vermeesch, 2013). Consistent with the sample KDEs, the MDS map shows more overlap between the Yarlung, Yigong, and Parlung zircon distributions compared to the distribution from the Namche Barwa cirque sample—and supports that the Tsangpo Gorge detrital zircon signal is distinct from other sedimentary sources in the drainage. The modern Siang River and 2000 Yigong flood deposit compilations plot close together, reflecting the similarity of their KDEs. The 1900 Yigong flood sample is close to but not directly linked to the 2000 flood compilation, highlighting the potential for significant variability among detrital age distributions for very similar outburst flood events sourced from the same location.

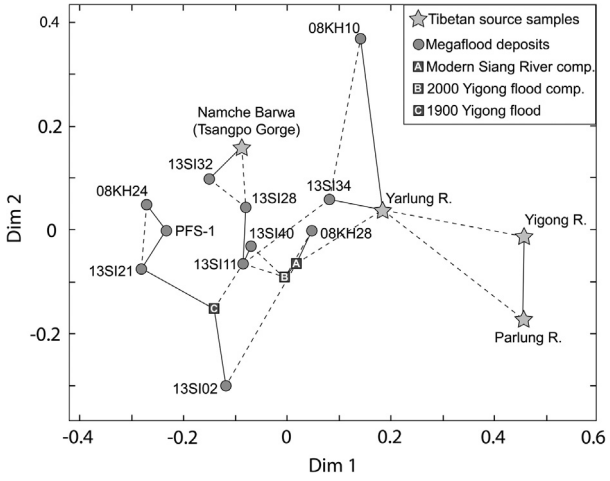

Fig. 5. MDS map displaying dissimilarity between four source samples used in previous studies shown in Fig. 3 (Yarlung River, Namche Barwa Cirque, Yigong River, and Parlung River), modern Siang River and 2000 Yigong flood compilations, the 1900 Yigong flood sample, and all individual megaflood deposits (Stress value = 0.10283). Solid lines between samples represent the most similar neighbor, whereas a dotted line is the second most similar. The distance in the x and y direction on this plot is in the unit of a KS statistic, so more dissimilar samples plot further apart on the 2D map.

Further insight from MDS analysis is limited. The MDS map is relatively insensitive to the positions of small age peaks observed in the different sample distributions. For example, samples 13SI32 and 13SI28 have prominent zircon age peaks from ~100-220 Ma, yet they plot nearest to the Namche Barwa source sample, which lacks these defined age peaks. In addition, comparing large and small n samples on an MDS map can be problematic (Vermeesch and Garzanti, 2015), so we evaluated the effects of sample size using a bootstrap approach. When we randomly remove 20% of the grains and re-compute the MDS map, we find in many iterations that the positions and connections among the samples vary. For example, a connection between PFS-1 and 13SI32 appears in several iterations (Fig. S10) that is not present in the original map (Fig. 5), yet we group these two samples based on the similarity of their KDEs (Fig. 4). Together, these observations suggest the large difference in sample size between megaflood deposits and some source samples makes the MDS map of limited use for interpreting zircon provenance.

4.3. BayesMix age component results

BayesMix inversion (Fig. 6, Table 3) identifies age components consistent with a ~50 Ma peak representing Tibetan source sediment in all sample compilations, but in varying proportions. The youngest age component in the modern Siang River and 2000 Yigong Flood sample compilations, respectively, represents 30-32% of the zircons, whereas the youngest component in the megaflood compilation represents 22% of the zircons. The next largest age components by proportion are consistent with ~350-550 Ma Himalayan ages from the Tsangpo Gorge area. Components in the 350-550 Ma range are identified in smaller proportions in the modern Siang River and 2000 Yigong flood compilations (23-24%) compared to the megaflood compilation (37%). The two age components in this range that are resolved in the megaflood compilation have means at 391 Ma and 475 Ma, corresponding to peaks in the Namche Barwa source sample. The BayesMix model identifies age components in the 50 to 350 Ma age range for the megaflood sample compilation that are not observed in the modern Siang River and Yigong flood deposit compilations.

Table 3
Results from BayesMix inversions.

Compilation	Modern Siang River samples (n=356)			2000 Yigong flood samples (n=387)			Megafloods (n=1608)			Group 1 (n=721)			Group 2 (n=418)			Group 3 (n=380)		
Sample names	*S32808-36, TUTING, S032508-16, PASIGHAT*			*08KH15, 08KH05, 08KH31, 08KH34, 13SI17*			*08KH10, 13SI34, 13SI11, 13SI40, 13SI02, 13SI28, 08KH28, 13SI32, 13SI21, 08KH24, PFS-1*			*08KH10, 13SI34, 13SI11, 13SI40*			*13SI21, PFS-1, 13SI32*			*13SI28, 08KH28, 13SI02*		
Component	Mean (Ma)	Error (Ma)	(%)	Mean (Ma)	Error (Ma)	(%)	Mean (Ma)	Error (Ma)	(%)	Mean (Ma)	Error (Ma)	(%)	Mean (Ma)	Error (Ma)	(%)	Mean (Ma)	Error (Ma)	(%)
1	53	12.6	30.0	66	15.7	31.8	54.8	9.5	22.4	41.6	8.6	40.0	17.9	22.6	11.7	28.2	3.4	5.2
2	112.1	2.4	3.4	196.5	8.6	6.3	90	4.6	0.7	238.6	95.4	8.7	128.0	6.7	0.7	45.2	11.9	17.1
3	199.4	27.2	3.6	477.1	21.3	23.1	129.6	8.4	2.1	469.1	5.1	24.7	206.4	7.9	3.0	114.1	7.5	1.3
4	482.2	19.6	24.0	766.2	7.8	1.9	220.1	3.2	3.5	978.9	10.0	4.2	437.0	22.3	15.7	142.2	13.4	1.2
5	817.1	7	6.8	1094.7	114.2	13.0	275	8.9	1.5	1214.1	9.6	8.8	471.9	4.5	34.8	213.9	4.7	10.2
6	1008.7	13.2	3.1	1151.3	31.9	8.8	443.1	65.3	14.8	1855.8	53.7	8.5	835.3	61.2	6.5	414.8	5.5	1.7
7	1155	6.9	12.6	1563.4	111.2	15.1	478.1	3.7	22.7	1619.7	5.1	3.6	991.4	4.7	6.9	482.1	2.4	20.3
8	1597.4	45.4	10.6	-	-	-	697.8	5.1	0.8	2494.9	64.9	1.1	1202.1	17.4	7.5	692.7	204.0	15.7
9	2900.9	12.2	4.1	-	-	-	834.1	4.3	3.6	2865.3	9.6	0.5	1305.4	7.0	0.1	1006.7	11.4	5.6
10	3227.1	8.1	0.6	-			1007.9	7.3	4.7	-	-	-	1726.2	57.0	13.2	1186.2	4.3	9.4
11	3529.2	24.4	1.2	-	-	-	1133.2	171.4	9.0	-	-	-	-	-	-	1349.6	43.4	5.5
12	-	-	-	-	-	-	1176	4.7	6.4	-	-	-	-	-	-	1608.8	33.7	5.2
13	-	-	-	-	-	-	1615.6	45.3	7.5	-	-	-	-	-	-	2849.5	15.7	0.1
14	-	-	-	-	-	-	2861.6	24.2	0.5	-	-	-	-	-	-	-	-	-

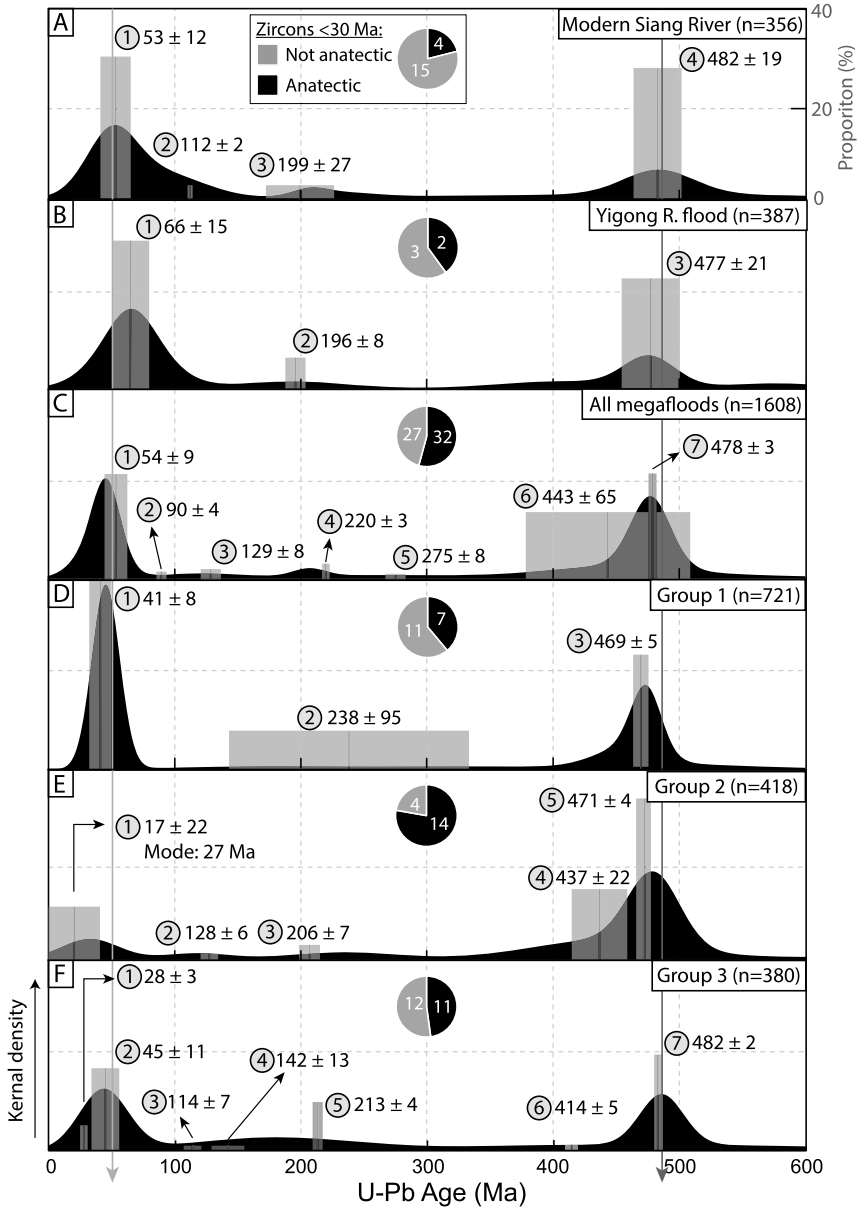

Fig. 6. Age components <600 Ma identified with BayesMix inversion of (a) modern Siang River sample, (b) 2000 Yigong flood sample compilation, (c) megaflood compilation, and (d-f) megaflood subgroups 1-3.

BayesMix inversion of the zircon data for sample groups 1, 2 and 3 show differences in the position and magnitude of the age components in each group (Table 3, Fig. 6). Prominent age components at ~41 Ma and ~45 Ma in group 1 and group 3 samples represent 40% and 17% of the zircons in each group, respectively; these age components overlap the diagnostic ~50 Ma peak from the Yarlung River source samples, although the positions of peaks in some individual samples varies and may be consistent with other sources. In contrast, the youngest age component in the group 2 samples comprising 11% of zircons with a mode at 27 Ma is consistent with the ≤30 Ma ages seen in the Namche Barwa source sample. The relative contribution from 350-550 Ma Himalayan rock from the Tsangpo Gorge area varies among individual samples, but on average these components make up 22-24% of zircons in groups 1 and 3, and 49% of group 2 zircons. Taken together, the BayesMix results highlight prominent Himalayan and Tibetan age components in the sample data, which we relate to zircon source areas below.

5. Discussion

Here we interpret zircon data from 11 megaflood deposits in the context of the zircon age distributions from potential source areas in Tibet, modern Siang River sediments, and historical outburst flood deposits. Floodwaters may entrain impounded lake sediment, material eroded from the hillslopes and channel during a flood event, and reworked sediment from previous lake/flood/fluvial deposits along the flood pathway—recording contributions from each of these sources in the zircon age distributions they deposit. Most of the megaflood deposit age distributions indicate zircon provenance from areas at or to the west of Namche Barwa in the Yarlung River drainage, or from Himalayan rocks of the Tsangpo Gorge. These data (1) suggest most of the megafloods that produced the sampled deposits were sourced from impoundments at or to the west of Namche Barwa in the Yarlung River drainage, and (2) suggest preferential erosion of the Tsangpo Gorge area during most of the recorded megaflood events in comparison to the modern river monsoonal and century-flood discharges, supporting

the hypothesis that megafloods may have had a disproportionately large impact on Gorge exhumation.

5.1. Zircon provenance and constraints on megaflood sources

There is widespread evidence of glacial-moraine dams in the eastern Himalaya, but it is unclear which potential sources of zircons are represented in the Siang River valley megaflood deposits. Lang et al. (2013) suggested that the megafloods that produced these deposits were sourced from glacially-impounded lakes in western Tibet because of the extensive record of lacustrine deposits on the Yarlung River adjacent to and upstream of Namche Barwa (Montgomery et al., 2004; Liu et al., 2006; 2015; 2018; Kaiser et al., 2010; Zhu et al., 2013; 2014; Huang et al., 2014; Chen et al., 2016). Recent observations of coarse sediments and bed forms in the middle-reaches of the Yarlung River provide evidence of megafloods sourced from impoundments even further to the west (Hu et al., 2018). Limited evidence also exists for paleo-lake deposits on the Yigong and Parlung Rivers in eastern Tibet (Guangxiang and Qingli, 2012), raising the question of whether megafloods were sourced from glacial impoundments in this area.

Outburst floods may be highly erosive at and immediately downstream of the dam breach (O'Connor and Beebee, 2009; Turzewski et al., 2019), entraining impounded lake sediment and/or dam, hillslope, and fluvial material near the source. Zircons from the dammed area may therefore be well represented in flood deposits downstream, as is observed for slackwater deposits of the 1900 and 2000 Yigong River floods (Lang et al., 2013; this study). Distinctive age peaks <250 Ma from potential megaflood source areas to the east and west of Namche Barwa in Tibet appear in varying proportions in the megaflood slackwater deposits, and have the potential to constrain the source areas of megafloods that produced the Siang River valley slackwater deposits.

Most of the megaflood deposits contain a strong western Tibetan source signature. The four megaflood deposits in group 1 (Fig. 4a) and sample 08KH24 (Fig. 4b) contain a prominent ~50 Ma peak characteristic of a Yarlung River source and generally lack other significant <600 Ma zircon peaks, except for the ~490 Ma Himalayan age component present in all flood deposits in this study. The three megaflood deposits in group 2 (Fig. 4c) contain a significant proportion of zircons that appear to have been sourced from the Namche Barwa massif/Tsangpo Gorge specifically, with a peak at ~27 Ma and a very large contribution of zircons at 350-550 Ma (Fig. 3e). Two of the group 3 deposits (08KH28, 13SI28; Fig. 4d) also have prominent $\leq$ 50 Ma age peaks indicative of Yarlung catchment/Namche Barwa provenance. These clear Yarlung River and Namche Barwa zircon provenance signals provide strong evidence that all eight group 1 and 2 deposits, and two of the group 3 deposits, record megafloods sourced from impoundments at or to the west of Namche Barwa that would have traversed the Yarlung River pathway through the Tsangpo Gorge.

Only one of the megaflood deposits (13SI02) may be compatible with an eastern Tibetan flood source (Fig. 4d). The youngest age peak at ~66 Ma and significant contribution of ~100-220 Ma zircons in deposit 13SI02 are similar to the zircon signals found in the Yigong and Parlung River source and the 1900 and 2000 Yigong flood samples and may be compatible with an impounded lake source to the east of Namche Barwa, although the age distribution of sample 13SI02 is poorly resolved. The other two group 3 deposits that show a significant contribution of $\leq$ 50 Ma zircons indicative of Yarlung catchment/Namche Barwa provenance (08KH28, 13SI28) also contain zircons in the ~100-220 Ma age range, which may be consistent with eastern Tibetan sources and/or flood-transported or reworked sediment that originated in the middle reaches of the Yarlung River. However, given that the youngest zircon age peak in these samples is significantly younger than 66 Ma, the impoundments that sourced the depositing floods were likely located west of Namche Barwa in the Yarlung drainage.

Diagnostic age peaks from multiple flood source areas are present in most of the flood deposits, showing the extent to which outburst floods rework previous flood and/or fluvial deposits. The 2000 Yigong flood deposit data show that a flood sourced from this eastern Tibetan tributary impoundment contains ~100-220 Ma zircons that characterize the eastern tributary source regions as well as ~50 Ma zircons characteristic of western Tibetan sources, similar to modern Siang River sediment (Fig. 4e, f). Several of the group 1 and group 2 megaflood deposits from western Tibetan sources contain age peaks that are diagnostic of source areas in the middle reaches of the Yarlung drainage. It is not possible to tell whether zircons with these diagnostic ages were entrained from their source area directly during the flood that produced the sampled deposit, or reworked from the deposits of a previous flood event. Nevertheless, the zircon ages may be consistent with provenance from impoundments on the middle Yarlung River (e.g., the Dazhuka-Yueju Gorge; Fig. 1) or tributaries to the Yarlung. Despite contributions to the zircon age signals of sediment reworking, our data show that the sediment preserved in megaflood slackwater deposits mostly comes from the western Tibetan sources within the Yarlung River drainage and from Namche Barwa/the Tsangpo Gorge—suggesting that these areas were where impounded lakes that sourced the megafloods were located.

Our data link most slackwater megaflood deposits to glacially impounded lake sources to the west of Namche Barwa, which is not surprising given the difference in valley morphology of the eastern and western drainages. Widespread glacial advances are dated throughout the region from 11-30 ka (Owen and Benn, 2005; Korup and Montgomery, 2008; Hu et al., 2017), including eastern Tibetan tributaries of the Yigong and Parlung River (Guangxiang and Qingli, 2012) that could result in glacial-moraine damming and lake impoundment. Glacial-moraine damming might produce smaller lakes in the eastern catchments compared to the Yarlung River catchment to the west of Namche Barwa because there is limited accommodation space for large (>10 km^3) lakes in these high-relief, narrow eastern tributaries. Indeed, the only mapped evidence of lacustrine sediments from glacial-impounded lakes exists in the Songzong sub-basin of the Parlung River catchment, which has a total area of only 16 km^2 (Guangxiang and Qingli, 2012). The area of the Songzong sub-basin is dwarfed by the areas of the Yarlung River sub-basins to the west of Namche Barwa (Fig. 1, 3). If the morphology of the Parlung and Yigong basins did not facilitate the formation of large glacially impounded lakes, this might explain why there is little evidence of megafloods from these tributaries in slackwater megaflood deposits along the Siang River.

5.2. Preferential erosion and sediment evacuation from the Tsangpo Gorge during megafloods

Our findings bear on the use of zircon age distributions as tracers of sediment sources and proxies for spatial patterns of erosion in the eastern Himalaya. Variation in source rock zircon fertility may bias comparisons of erosion rate or sediment flux estimates and is important to account for in studies comparing erosion rates across different drainage areas (Vezzoli et al., 2016; Braun et al., 2018). Like Lang et al. (2013), we avoid this bias by comparing deposits within the same drainage area, with the same potential source rocks. We assume that source rock zircon fertility did not change significantly over the Quaternary, and that the best explanation for changes in the zircon age distributions is changes in the relative contribution of zircons from different locations within the source area.

Lang et al. (2013) found a disproportionate amount of zircons from the Tsangpo Gorge in megaflood slackwater deposits compared to Yigong flood deposits and modern Siang River sediments, and used this result to argue that megafloods preferentially focus erosion in the Gorge. Our analyses of 1438 zircons from seven additional megaflood deposits brings the total observations to 11 deposits and n=1608 zircon data, which confirm that on average the megaflood samples do have a higher proportion of zircons derived from the Gorge compared to the modern Siang River and Yigong flood samples. However, our large dataset also shows significant variation among the zircon age distributions of individual megaflood deposits. Section 5.1 discussed the potential contributions to zircon provenance and age distributions of flood impoundment location and sediment reworking; here we explore the degree to which the age distributions reflect the spatial pattern of erosion during a flood event.

Megafloods that we interpret to have come from failed glacial moraine impoundments on the flanks of Namche Barwa just upstream of the Tsangpo Gorge (group 2) have the greatest contribution (~49%) of ~490 Ma zircons and anatectic zircons characteristic of Himalayan rock from the Tsangpo Gorge area in their deposits. We do not know how many of these zircons were eroded from the Gorge area during vs. prior to the megafloods that produced the sampled deposits. However, these megaflood deposits contain about twice as many ~490 Ma zircons as is observed in 2000 Yigong flood and modern Siang River deposits, and significantly more ~490 Ma zircons than are found in all but one of the other flood deposits (08KH24), indicating that sediment reworking cannot explain the bulk of this signal. Outburst floods sourced from impoundments at Namche Barwa would be expected to focus erosion near the breach, eroding and entraining a disproportionate amount of material in the Gorge area. We suggest the simplest interpretation is that the great abundance of Himalayan and anatectic zircons in these deposits does reflect preferential erosion in the Tsangpo Gorge.

Varying proportions of Gorge-sourced zircons in the other megaflood samples are more difficult to interpret, but nevertheless support the idea that megafloods preferentially eroded and entrained material from the Tsangpo Gorge area compared to modern river flows. Individual megaflood sample age distributions vary due to factors like impoundment location and sediment recycling, making it impossible to quantify the specific percent contribution to the Gorge-sourced zircon signal due to erosion from the depositing megaflood. It is also possible that some of the ~490 Ma zircons may have been derived from Himalayan rocks that crop out in northward-draining tributaries to the Yarlung upstream of the Gorge. Fission-track double dating of these zircons to further refine their provenance (Lang et al., 2016) is beyond the scope of this study. However, the megaflood samples also contain a higher proportion of <30 Ma anatectic zircons eroded directly from the Gorge compared to the modern Siang River samples (Fig. 6), providing independent provenance constraints. Thus despite these complications, the data indicate 9 of the 11 megaflood deposits contain significantly more zircons sourced from the Tsangpo Gorge compared to modern Siang River sediments (Fig. 4), providing strong evidence that megafloods are capable of focusing erosion in the Gorge. This finding combined with evidence indicating that most of these megafloods were probably sourced from impoundments in the Yarlung River drainage at or to the west of Namche Barwa, highlight the potential for repeated megafloods to influence the morphology of the Yarlung-Po River pathway through the Tsangpo Gorge—and support the hypothesis that preferential erosion of the Tsangpo Gorge during megafloods may have been an important mechanism for keeping pace with rapid rock uplift during the Quaternary.

6. Conclusions

We presented new detrital zircon U-Pb geochronology data for outburst flood slackwater deposits preserved downstream of the Tsangpo Gorge, that combined with previous zircon data for Tibetan source regions and downstream fluvial and outburst flood deposits shed light on the sources and erosional impact of Quaternary megafloods in the eastern Himalayan syntaxis. Despite complications due to the entrainment of previously deposited sediment along the flood pathway, the flood slackwater deposits contain clear zircon provenance signals that we interpret to reflect impounded lake sources and spatial patterns of erosion during floods:

- Diagnostic $\leq$250 Ma age components in the studied deposits indicate that most megaflood events were sourced from impoundments in the Yarlung River drainage at or to the west of Namche Barwa, with some sample ages suggesting provenance potentially as far upstream as the middle Yarlung.
- Only one of the eleven studied megaflood deposits may be compatible with an eastern Tibetan source on the Yigong and Parlung Rivers. It is possible that limited accommodation space for large (>10 km^3) lakes in the high-relief, narrow valleys of the Parlung and Yigong drainages may explain the paucity of evidence for megafloods from eastern Tibetan sources in our dataset.
- Our analyses of n=1139 zircons from 7 new megaflood deposits add significantly to the available data documenting floods through the Tsangpo Gorge, and show that megaflood deposits contain a disproportionate amount of zircons from the Gorge compared to the modern Siang River and historical Yigong flood deposits. The overabundance of Gorge-sourced zircons is unlikely to be explained by sediment reworking alone, and provides evidence that megafloods preferentially focused erosion in the Gorge.
- The highest proportions of Gorge-sourced zircons are found in deposits from megafloods that we interpret to have been sourced from glacial-moraine dam impoundments on the flanks of Namche Barwa, immediately upstream of the Tsangpo Gorge. This finding highlights the potential for outburst flood source location to control erosion patterns by focusing erosion at and immediately downstream of the dam breach.

Taken together, our findings place new constraints on megaflood source locations and processes of sediment reworking that influence downstream zircon age distributions, and show that megafloods had the potential to preferentially erode the Tsangpo Gorge and contribute substantially to rapid exhumation of the eastern Himalayan syntaxis.

Declaration of competing interest

The authors declare that they have no known competing financial interests or personal relationships that could have appeared to influence the work reported in this paper.

Acknowledgements

We thank Oken Tayeng, Tapir Tayeng and Abor Travels for field support. We acknowledge David Montgomery, Alison Duvall, and Megan Mueller for commenting on earlier drafts. Thank you to Paul O'Sullivan at GeoSep Services who aided with mineral separations, and Mariah Danner for assistance in the laboratory and with zircon analyses. We also thank the Arizona LaserChron Center for performing zircon analyses and assistance with data reduction. Funding was provided by the Quaternary Research Center at the University of Washington and U.S. National Science Foundation (EAR-1349279 and EAR-0955309 to KWH).

Appendix A. Supplementary material

Supplementary material related to this article can be found online at https://doi.org/10.1016/j.epsl.2020.116113.

References

Amidon, W.H., Burbank, D.W., Gehrels, G.E., 2005. U–Pb zircon ages as a sediment mixing tracer in the Nepal Himalaya. Earth Planet. Sci. Lett. 235 (1–2), 244–260.

Booth, A.L., Chamberlain, C.P., Kidd, W.S., Zeitler, P.K., 2009. Constraints on the metamorphic evolution of the eastern Himalayan syntaxis from geochronologic and petrologic studies of Namche Barwa. Geol. Soc. Am. Bull. 121 (3–4), 385–407.

Booth, A.L., Zeitler, P.K., Kidd, W.S.F., Wooden, J., Liu, Y., Idleman, B., Hren, M., Chamberlain, C.P., 2004. U-Pb zircon constraints on the tectonic evolution of southeastern Tibet, Namche Barwa Area. Am. J. Sci. 304, 889–929. https://doi.org/10.2475/ajs.304.10.889.

Botev, Z.I., Grotowski, J.F., Kroese, D.P., 2010. Kernel density estimation via diffusion. Ann. Stat. 38 (5), 2916–2957.

Braun, J., Gemignani, L., Beek, P.V.D., 2018. Extracting information on the spatial variability in erosion rate stored in detrital cooling age distributions in river sands. Earth Surf. Dyn. 6 (1), 257–270.

Burrard, S.G., Hayden, H.H., 1907. A Sketch of the Geography and Geology of the Himalaya Mountains and Tibet (Vol. 1). Superintendent government printing, India.

Chen, Y., Aitchison, J.C., Zong, Y., Li, S.H., 2016. OSL dating of past lake levels for a large dammed lake in southern Tibet and determination of possible controls on lake evolution. Earth Surf. Process. Landf. 41 (11), 1467–1476.

Cina, S.E., Yin, A., Grove, M., Dubey, C.S., Shukla, D.P., Lovera, O.M., Foster, D.A., 2009. Gangdese arc detritus within the eastern Himalayan Neogene foreland basin: implications for the Neogene evolution of the Yalu-Brahmaputra River system. Earth Planet. Sci. Lett. 285 (1–2), 150–162.

Delaney, K.B., Evans, S.G., 2015. The 2000 Yigong landslide (Tibetan Plateau), rockslide-dammed lake and outburst flood: review, remote sensing analysis, and process modelling. Geomorphology 246, 377–393. https://doi.org/10.1016/j.geomorph.2015.06.020.

Enkelmann, E., Ehlers, T.A., Zeitler, P.K., Hallet, B., 2011. Denudation of the Namche Barwa antiform, eastern Himalaya. Earth Planet. Sci. Lett. 307 (3–4), 323–333.

Gallagher, K., Charvin, K., Nielsen, S., Sambridge, M., Stephenson, J., 2009. Markov chain Monte Carlo (MCMC) sampling methods to determine optimal models, model resolution and model choice for earth science problems. Mar. Pet. Geol. 26, 525–535. https://doi.org/10.1016/j.marpetgeo.2009.01.00.

Galy, V., Peucker-Ehrenbrink, B., Eglinton, T., 2015. Global carbon export from the terrestrial biosphere controlled by erosion. Nature 521 (7551), 204.

Gehrels, G., Kapp, P., Decelles, P., Pullen, A., Blakey, R., Weislogel, A., Ding, L., Guynn, J., Martin, A., McQuarrie, N., Yin, A., 2011. Detrital zircon geochronology of pre-Tertiary strata in the Tibetan-Himalayan orogen. Tectonics 30 (5), 5016. https://doi.org/10.1029/2011TC002868.

Goswami, D.C., 1985. Brahmaputra River, Assam, India: physiography, basin denudation, and channel aggradation. Water Resour. Res. 21 (7), 959–978. https://doi.org/10.1029/WR021i007p00959.

Guangxiang, Y., Qingli, Z., 2012. Glacier-dammed lake in southeastern Tibetan Plateau during the Last Glacial Maximum. J. Geol. Soc. India 79 (3), 295–301.

Hu, H.P., Feng, J.L., Chen, F., 2017. δ^{18}O and δ^{13}C in fossil shells of Radix sp. from the sediment succession of a dammed palaeo-lake in the Yarlung Tsangpo valley, Tibet, China. Boreas 46 (3), 412–427. https://doi.org/10.1111/bor.12231.

Hu, H.P., Feng, J.L., Chen, F., 2018. Sedimentary records of a palaeo-lake in the middle Yarlung Tsangpo: implications for terrace genesis and outburst flooding. Quat. Sci. Rev. 192, 135–148. https://doi.org/10.1016/j.quascirev.2018.05.037.

Huang, S.Y., Chen, Y.G., Burr, G.S., Jaiswal, M.K., Lin, Y.N., Yin, G., Liu, J., Zhao, S., Cao, Z., 2014. Late Pleistocene sedimentary history of multiple glacially dammed lake episodes along the Yarlung-Tsangpo river, southeast Tibet. Quat. Res. 82 (2), 430–440.

Jasra, A., Stephens, D., Gallagher, K., Holmes, C., 2006. Bayesian mixture modelling in geochronology via Markov chain Monte Carlo. Math. Geol. 38, 269–300. https://doi.org/10.1007/s11004-005-9019-3.

Kaiser, K., Lai, Z., Schneider, B., Junge, F.W., 2010. Late Pleistocene genesis of the middle Yarlung Zhangbo Valley, southern Tibet (China), as deduced by sedimentological and luminescence data. Quat. Geochronol. 5 (2–3), 200–204.

Korup, O., Montgomery, D.R., 2008. Tibetan plateau river incision inhibited by glacial stabilization of the Tsangpo gorge. Nature 455 (7214), 786–789. https://doi.org/10.1038/nature07322.

Korup, O., Montgomery, D.R., Hewitt, K., 2010. Glacier and landslide feedbacks to topographic relief in the Himalayan syntaxes. Proc. Natl. Acad. Sci. USA 107 (12), 5317–5322. https://doi.org/10.1073/pnas.0907531107.

Lamb, M., Dietrich, W., Aciego, S., Depaolo, D., Manga, M., 2008. Formation of Box Canyon, Idaho, by megaflood: implications for seepage erosion on Earth and Mars. Science 320 (5879), 1067–1070. https://doi.org/10.1126/science.1156630.

Lamb, M., Fonstad, M., 2010. Rapid formation of a modern bedrock canyon by a single flood event. Nat. Geosci. 3 (7), 477–481. https://doi.org/10.1038/NGEO894.

Lang, K.A., Huntington, K.W., 2014. Antecedence of the Yarlung–Siang–Brahmaputra River, eastern Himalaya. Earth Planet. Sci. Lett. 397, 145–158. https://doi.org/10.1016/j.epsl.2014.04.026.

Lang, K.A., Huntington, K.W., Montgomery, D.R., 2013. Erosion of the Tsangpo Gorge by megafloods, Eastern Himalaya. Geology 41 (9), 1003–1006.

Lang, K.A., Huntington, K.W., Burmister, R., Housen, B., 2016. Rapid exhumation of the eastern Himalayan syntaxis since the Late Miocene. Geol. Soc. Am. Bull. 128. https://doi.org/10.1130/B31419.1.

Larsen, I.J., Lamb, M., 2016. Progressive incision of the Channeled Scablands by outburst floods. Nature 538 (7624), 229–232. https://doi.org/10.1038/nature19817.

Larsen, I.J., Montgomery, D.R., 2012. Landslide erosion coupled to tectonics and river incision. Nat. Geosci. 5 (7), 468–473. https://doi.org/10.1038/NGEO1479.

Licht, A., Pullen, A., Kapp, P., Abell, J., Giesler, N., 2016. Eolian cannibalism: reworked loess and fluvial sediment as the main sources of the Chinese Loess Plateau. Geol. Soc. Am. Bull. 128 (5–6), 944–956.

Liu, W., Lai, Z., Hu, K., Ge, Y., Cui, P., Zhang, X., Liu, F., 2015. Age and extent of a giant glacial-dammed lake at Yarlung Tsangpo gorge in the Tibetan Plateau. Geomorphology 246, 370–376.

Liu, Y., Montgomery, D.R., Hallet, B., Tang, W., Zhang, J.L., Zhang, X.Y., 2006. Quaternary glacier blocking events at the entrance of Yarlung Zangbo Great Canyon, Southeast Tibet. Quat. Sci. 26 (1), 52–62.

Liu, W., Zhou, G.G., Ge, Y., Huang, R., 2018. Gradual late stage deepening of Gega ice-dammed lake, Tsangpo gorge, southeastern Tibet, indicated by preliminary sedimentary rock magnetic properties. Acta Geophys., 1–8.

Makuluni, P., Kirkland, C.L., Barham, M., 2019. Zircon grain shape holds provenance information: a case study from southwestern Australia. Geol. J. 54 (3), 1279–1293.

Montgomery, D.R., Hallet, B., Yuping, L., Finnegan, N., Anders, A., Gillespie, A., Greenberg, H.M., 2004. Evidence for Holocene megafloods down the Tsangpo River gorge, southeastern Tibet. Quat. Res. 62 (2), 201–207. https://doi.org/10.1016/j.yqres.2004.06.008.

O'Connor, J.E., Beebee, R.A., 2009. Floods from natural rock-material dams. In: Carling, P.A., Baker, V.R., Burr, DM (Eds.), Megaflooding on Earth and Mars. Cambridge University Press, Cambridge, pp. 128–171.

O'Connor, J.E., Clague, J.J., Walder, J.S., Manville, V., Beebee, R.A., 2013. Outburst floods. In: Shroder, J.F. (Ed.), Treatise on Geomorphology, vol. 9, pp. 475–510.

Owen, L.A., Benn, D.I., 2005. Equilibrium-line altitudes of the Last Glacial Maximum for the Himalaya and Tibet: an assessment and evaluation of results. Quat. Int. 138–139, 55–78.

Perron, J. Taylor, Venditti, Jeremy G., 2016. Earth science: megafloods downsized. Nature 538 (7624), 174–175.

Perrot, M., Tremblay, A., David, J., 2017. Detrital zircon U-Pb geochronology of the Magog Group, southern Quebec – stratigraphic and tectonic implications for the Quebec Appalachians. Am. J. Sci. 317 (10), 1049–1094. https://doi.org/10.2475/10.2017.01.

Pullen, A., Ibáñez-Mejía, M., Gehrels, G.E., Ibáñez-Mejía, J.C., Pecha, M., 2014. What happens when n=1000? Creating large-n geochronological datasets with LA-ICP-MS for geologic investigations. J. Anal. At. Spectrom. 29 (6), 971–980.

Shang, Y., Yang, Z., Li, L., Liu, D., Liao, Q., Wang, Y., 2003. A super-large landslide in Tibet in 2000: background, occurrence, disaster, and origin. Geomorphology 54 (3–4), 225–243.

Sircombe, K.N., Stern, R.A., 2002. An investigation of artificial biasing in detrital zircon U-Pb geochronology due to magnetic separation in sample preparation. Geochim. Cosmochim. Acta 66 (13), 2379–2397.

Srivastava, P., Kumar, A., Chaudhary, S., Meena, N., Sundriyal, Y.P., Rawat, S., Rana, N., Perumal, R.J., Bisht, P., Sharm, D., Agnihotri, R., Bagri, D.S., Juyal, N., Wasson, R.J., Ziegler, A.D., 2017. Paleofloods records in Himalaya. Geomorphology 284, 17–30. https://doi.org/10.1016/j.geomorph.2016.12.011.

Stewart, R.J., Hallet, B., Zeitler, P.K., Malloy, M.A., Allen, C.M., Trippett, D., 2008. Brahmaputra sediment flux dominated by highly localized rapid erosion from the easternmost Himalaya. Geology 36 (9), 711–714.

Turowski, J.M., Hovius, N., Meng-Long, H., Lague, D., Men-Chiang, C., 2008. Distribution of erosion across bedrock channels. Earth Surf. Process. Landf. 33, 353–363. https://doi.org/10.1002/esp.1559.

Turzewski, M.D., Huntington, K.W., LeVeque, R.J., 2019. The geomorphic impact of outburst floods: integrating observations and numerical simulations of the 2000 Yigong flood, eastern Himalaya. J. Geophys. Res., Earth Surf. 124. https://doi.org/10.1029/2018JF004778.

Vermeesch, P., 2013. Multi-sample comparison of detrital age distributions. Chem. Geol. 341, 140–146.

Vermeesch, P., 2018. Dissimilarity measures in detrital geochronology. Earth-Sci. Rev. 178, 310–321. https://doi.org/10.1016/j.earscirev.2017.11.027.

Vermeesch, P., Garzanti, E., 2015. Making geological sense of "Big Data" in sedimentary provenance analysis. Chem. Geol. 409, 20–27. https://doi.org/10.1016/j.chemgeo.2015.05.004.

Vermeesch, P., Rittner, M., Petrou, E., Omma, J., Mattinson, C., Garzanti, E., 2017. High throughput petrochronology and sedimentary provenance analysis by automated phase mapping and LAICPMS. Geochem. Geophys. Geosyst. 18 (11), 4096–4109.

Vezzoli, G., Garzanti, E., Limonta, M., Andò, S., Yang, S., 2016. Erosion patterns in the Changjiang (Yangtze River) catchment revealed by bulk-sample versus single-mineral provenance budgets. Geomorphology 261, 177–192.

Whipple, K.X., Dibiase, R.A., Crosby, B.T., 2013. Bedrock rivers. In: Treatise on Geomorphology. Elsevier Inc., pp. 550–573.

Zhang, J.Y., Yin, A., Liu, W.C., Ding, L., Xu, X.M., 2016. First geomorphological and sedimentological evidence for the combined tectonic and climate control on Quaternary Yarlung river diversion in the eastern Himalaya. Lithosphere 8 (3), 293–316.

Zhang, J.Y., Yin, A., Liu, W.C., Wu, F.Y., Lin, D., Grove, M., 2012. Coupled U-Pb dating and Hf isotopic analysis of detrital zircon of modern river sand from the Yalu River (Yarlung Tsangpo) drainage system in southern Tibet: constraints on the transport processes and evolution of Himalayan rivers. Bull. Geol. Soc. Am. 124 (9–10), 1449–1473.

Zhu, S., Wu, Z., Zhao, X., Li, J., Xiao, K., 2014. Ages and genesis of terrace flights in the middle reaches of the Yarlung Zangbo River, Tibetan Plateau, China. Boreas 43 (2), 485–504.

Zhu, S., Wu, Z.H., Zhao, X.T., Wang, C.M., Xiao, K.Y., 2013. The age of glacial dammed lakes in the Yarlung Zangbo River Grand Bend during late Quaternary by OSL. Diqiu Xuebao (Acta Geoscientica Sinica) 34 (2), 246–250.